Engineering MEMS Resonators With Low Thermoelastic Damping

Amy Duwel, Rob N. Candler, Thomas W. Kenny, and Mathew Varghese

***Abstract*—This paper presents two approaches to analyzing and calculating thermoelastic damping in micromechanical resonators. The first approach solves the fully coupled thermomechanical equations that capture the physics of thermoelastic damping in both two and three dimensions for arbitrary structures. The second approach uses the eigenvalues and eigenvectors of the uncoupled thermal and mechanical dynamics equations to calculate damping. We demonstrate the use of the latter approach to identify the thermal modes that contribute most to damping, and present an example that illustrates how this information may be used to design devices with higher quality factors. Both approaches are numerically implemented using a finite-element solver (Comsol Multiphysics). We calculate damping in typical micromechanical resonator structures using Comsol Multiphysics and compare the results with experimental data reported in literature for these devices. [1595]**

NOMENCLATURE

Variable	Physical Definition
E	Young's modulus.
α	Coefficient of thermal expansion.
T_o	Nominal average temperature (300 K).
ρ	Density of solid.
$C_{\rm sp}$	Specific heat capacity of a solid.
C_v	Heat capacity of a solid $C_v = \rho C_{\rm sp}$.
κ	Thermal conductivity of a solid.
$\omega_{\rm mech}$	Mechanical resonance frequency.
τ_n	Characteristic time constant for thermal mode n.
σ	Stress.
ε	Strain.
λ, μ	Elastic Lamé parameters.
T	Temperature.
S	Entropy.
$[u \quad v \quad w]$	Components of displacement in x, y, and z directions respectively.
$\bar{u} = [u \quad v]$	2-D vector of mechanical displacements.
U_m	Mechanical mode amplitude.
$\bar{\Phi}_m$	Mechanical eigenmode shape function.
ω_m	Mechanical resonant frequency for eigenmode m.
A_n	Thermal mode amplitude .
T_n	Thermal eigenmode shape function .
ω_{th}	Characteristic frequency of dominant thermal mode.
ΔW	Energy lost from mechanical resonator system.
W	Energy stored in mechanical resonator.

Manuscript received May 7, 2005; revised April 12, 2006. This work was supported in part by DARPA HERMIT by ONR N66001-03-1-8942. Subject Editor L. W. Lin.

A. Duwel and M. Varghese are with the Charles Stark Draper Laboratory, Cambridge, MA 02139 USA (e-mail: aduwel@draper.com).

R. N. Candler and T. W. Kenny are with the Departments of Mechanical and Electrical Engineering, Stanford University, Stanford, CA 94305 USA.

Digital Object Identifier 10.1109/JMEMS.2006.883573

I. INTRODUCTION

MICROMECHANICAL resonators are used in a wide variety of applications, including inertial sensing, chemical and biological sensing, acoustic sensing, and microwave transceivers. Despite the distinct design requirements for each of these applications, a ubiquitous resonator performance parameter emerges. This is the resonator's Quality factor (Q), which describes the mechanical energy damping. In all applications, it is important to have design control over this parameter, and in most cases, it is invaluable to minimize the damping. Over the past decade, both experimental and theoretical studies [1]–[6], [9], [22] have highlighted the important role of thermoelastic damping (TED) in micromechanical resonators. However, the tools available to analyze and design around TED in typical micromechanical resonators are limited to analytical calculations that can be applied to relatively simple mechanical structures. These are based on the defining work done by Zener in [7], [8].

Zener developed general expressions for thermoelastic damping in vibrating structures, with the specific case study of a beam in its fundamental flexural mode. In [8], Zener's calculation was based on fundamental thermodynamic expressions for stored mechanical energy, work, and thermal energy that used *coupled* thermal-mechanical constitutive relations for stress, strain, entropy, and temperature. However, in order to evaluate these energy expressions for a specific resonator, Zener proposed that the strain and temperature solutions from *uncoupled dynamical equations* could be sufficient. He found the eigensolutions of the mechanical equation, and, separately, the eigensolutions of the uncoupled thermal equation. By applying these to the coupled thermodynamic energies, Zener calculated the thermoelastic Q of an isotropic homogenous resonator to be

$$Q^{-1} = \left(\frac{E\alpha^2 T_o}{C_v}\right) \sum_n \frac{\omega_{\rm mech}\tau_n}{1 + (\omega_{\rm mech}\tau_n)^2} f_n \qquad (1)$$

where the physical constants are listed in the Nomenclature, ω_{mech} is the mechanical resonance frequency and τ_n is the characteristic time constant of a given thermal mode. This takes into account the fact that multiple thermal modes may add to the damping of a single mechanical resonance. The contribution of a given mode, n, is determined by its weighting function, f_n.

Zener explicitly calculated the weighting functions for a simple beam resonating in its fundamental flexural mode. In order to make the analysis tractable, he assumed that only thermal gradients across the beam width (dimension in the direction of the flexing) were significant. This left only a 1D thermal equation to solve. Zener found that a single thermal mode dominated, giving

$$Q^{-1} = \left(\frac{E\alpha^2 T_o}{C_v}\right)\frac{\omega_{\mathrm{mech}}\tau}{1+\omega_{\mathrm{mech}}^2\tau^2}. \tag{2}$$

Few structures are amenable to the simplifications that led to (2) for Q. However, Zener's expression (1) is quite general. In Section III, we show how numerical solutions to the uncoupled mechanical and thermal dynamics of a resonator can be used to evaluate (1). This adds a great deal of power to Zener's approach, since arbitrary geometries can be considered.

We show how Zener's weighting function approach offers an intuition into the details of the energy transfer. At the same time, our results highlight the limits of intuition in identifying the thermal modes of interest. For example, we find that the simplification Zener made in assuming only thermal gradients in one direction along the beam were significant does not capture the most important thermal mode, even for a simple beam. In addition, past efforts to estimate Q without explicitly calculating the weighting functions have been shown [9] to greatly overestimate the damping behavior of real systems. This "modified" interpretation of Zener's method can be misleading.

In this paper, we describe a method for using full numerical solutions to evaluate Q using Zener's approach. We call this a "weakly coupled" approach. We also present our numerical method for solving the fully coupled thermoelastic dynamics equations to calculate Q for an arbitrary structure. Using numerical solutions in the weakly coupled approach offers powerful guidance in engineering around thermoelastic damping, while fully coupled solutions offer the ability to precisely evaluate and optimize the thermoelastic Q of a resonator.

II. Numerical Solution of the Fully Coupled TED Equations

The coupled equations governing thermoelastic vibrations in a solid are derived in [19]. Section II-A outlines the basic principles of this derivation. Section II-B highlights modifications required for a two–dimensional (2-D) plane stress formulation. The full 2D and 3D equations are written explicitly so that they are accessible to the user community. We numerically solve the 2- and 3-D dynamical equations using the finite-elements based package Comsol Multiphysics [11]. The Comsol implementation is described in [12] and [13]. This analysis can be applied to the wide variety of MEMS resonator structures reported in the literature. It is a useful tool for determining whether TED limits performance or whether other damping mechanisms, such as anchor damping [23], should be investigated instead. Section II-C demonstrates the application of TED simulations to a few example MEMS resonator structures. Quality factors are calculated and compared with the analytical (1) as well as with experimental measurements reported in the literature.

A. Governing Equations in 3-D

The constitutive relations for an isotropic thermoelastic solid, derived from thermodynamic energy functions, are in matrix form

$$\begin{bmatrix}\sigma_1\\ \sigma_2\\ \sigma_3\\ \sigma_4\\ \sigma_5\\ \sigma_6\end{bmatrix} = \begin{bmatrix}\lambda+2\mu & \lambda & \lambda & 0 & 0 & 0\\ \lambda & \lambda+2\mu & \lambda & 0 & 0 & 0\\ \lambda & \lambda & \lambda+2\mu & 0 & 0 & 0\\ 0 & 0 & 0 & \mu & 0 & 0\\ 0 & 0 & 0 & 0 & \mu & 0\\ 0 & 0 & 0 & 0 & 0 & \mu\end{bmatrix}\begin{bmatrix}\varepsilon_1\\ \varepsilon_2\\ \varepsilon_3\\ \varepsilon_4\\ \varepsilon_5\\ \varepsilon_6\end{bmatrix} - (3\lambda+2\mu)T\begin{bmatrix}\alpha\\ \alpha\\ \alpha\\ 0\\ 0\\ 0\end{bmatrix} \tag{3}$$

and

$$S = \begin{bmatrix}\alpha & \alpha & \alpha & 0 & 0 & 0\end{bmatrix} \times \begin{bmatrix}\lambda+2\mu & \lambda & \lambda & 0 & 0 & 0\\ \lambda & \lambda+2\mu & \lambda & 0 & 0 & 0\\ \lambda & \lambda & \lambda+2\mu & 0 & 0 & 0\\ 0 & 0 & 0 & \mu & 0 & 0\\ 0 & 0 & 0 & 0 & \mu & 0\\ 0 & 0 & 0 & 0 & 0 & \mu\end{bmatrix}\begin{bmatrix}\varepsilon_1\\ \varepsilon_2\\ \varepsilon_3\\ \varepsilon_4\\ \varepsilon_5\\ \varepsilon_6\end{bmatrix} + \frac{C_v}{T_o}T \tag{4}$$

where reduced tensor notation has been used, and the variables are defined in the Nomenclature.

To obtain the coupled dynamics, the constitutive relations are applied to the force balance constraints and Fourier's law of heat transfer. Force balance in the x-direction gives

$$\rho\frac{\partial^2 u}{\partial t^2} = \left(\frac{\partial\sigma_1}{\partial x} + \frac{\partial\sigma_5}{\partial y} + \frac{\partial\sigma_6}{\partial z}\right) \tag{5}$$

with similar relations for the y- and z-directions.

Substituting displacement for strain and simplifying, the 3-D equations of motion become

$$\begin{aligned}\rho\frac{\partial^2 u}{\partial t^2} =& \mu\left(\frac{\partial^2 u}{\partial x^2}+\frac{\partial^2 u}{\partial y^2}+\frac{\partial^2 u}{\partial z^2}\right)\\ &+(\lambda+\mu)\left(\frac{\partial^2 u}{\partial x^2}+\frac{\partial^2 v}{\partial x\partial y}+\frac{\partial^2 w}{\partial x\partial z}\right)\\ &-\alpha(3\lambda+2\mu)\frac{\partial T}{\partial x}\end{aligned} \tag{6}$$

$$\begin{aligned}\rho\frac{\partial^2 v}{\partial t^2} =& \mu\left(\frac{\partial^2 v}{\partial x^2}+\frac{\partial^2 v}{\partial y^2}+\frac{\partial^2 v}{\partial z^2}\right)\\ &+(\lambda+\mu)\left(\frac{\partial^2 u}{\partial y\partial x}+\frac{\partial^2 v}{\partial y^2}+\frac{\partial^2 w}{\partial y\partial z}\right)\\ &-\alpha(3\lambda+2\mu)\frac{\partial T}{\partial y}\end{aligned} \tag{7}$$

$$\rho\frac{\partial^2 w}{\partial t^2} = \mu\left(\frac{\partial^2 w}{\partial x^2}+\frac{\partial^2 w}{\partial y^2}+\frac{\partial^2 w}{\partial z^2}\right) + (\lambda+\mu)\left(\frac{\partial^2 u}{\partial z\partial x}+\frac{\partial^2 v}{\partial z\partial y}+\frac{\partial^2 w}{\partial z^2}\right) - \alpha(3\lambda+2\mu)\frac{\partial T}{\partial z}. \quad (8)$$

To obtain the thermal dynamics, we apply Fourier's law

$$T\dot{S} = \kappa\nabla^2 T. \quad (9)$$

The constitutive relations are applied, and the resulting equation is linearized around T_o, the ambient temperature, to give, in 3-D

$$\kappa\nabla^2 T - C_v\dot{T} - \alpha(3\lambda+2\mu)T_o\left(\frac{\partial\dot{u}}{\partial x}+\frac{\partial\dot{v}}{\partial y}+\frac{\partial\dot{w}}{\partial z}\right) = 0. \quad (10)$$

In summary, (6)–(8) and (10) form a set of coupled linear equations in 3-D. Since the equations are linear, we can use a finite elements based approach to solving them on an arbitrary geometry. We solve for the unforced eigenmodes. The generalized eigenvectors contain u, v, w, and T at every node. The eigenvalues, ω_i, are complex. The imaginary component represents the mechanical vibration frequency, while the real part provides the rate of decay for an unforced vibration due to the thermal coupling. The quality factor of the resonator is defined as

$$Q_i = \frac{\mathrm{Im}\{\omega_i\}}{2\mathrm{Re}\{\omega_i\}}. \quad (11)$$

B. Governing Equations in 2-D With Plane Stress Approximations

For long beams in flexural vibrations, we can identify one axis (we chose to be z) in which all strains are uniform and no loads are applied. For clarity, we define the *x* axis along the beam length and the *y* axis in the direction of flexing. Along the z-direction σ_3, σ_4,and σ_5 must be zero throughout the structure. This is essentially a plane stress approximation. When $\sigma_3 = 0$ is applied to (3) above, we find that

$$\varepsilon_3 = -\frac{\lambda}{\lambda+2\mu}(\varepsilon_1+\varepsilon_2) + \alpha\left(\frac{3\lambda+2\mu}{\lambda+2\mu}\right)T. \quad (12)$$

In the plane stress approximation, the force balance relation (5) is

$$\rho\frac{\partial^2 u}{\partial t^2} = \left(\frac{\partial\sigma_1}{\partial x}+\frac{\partial\sigma_6}{\partial y}\right). \quad (13)$$

Expanding the stress terms using the constitutive relations,

$$\rho\frac{\partial^2 u}{\partial t^2} = \lambda\frac{\partial}{\partial x}(\varepsilon_1+\varepsilon_2+\varepsilon_3) + 2\mu\frac{\partial}{\partial x}\varepsilon_1 + \mu\frac{\partial}{\partial y}\varepsilon_6 - \alpha(3\lambda+2\mu)\frac{\partial T}{\partial x}. \quad (14)$$

Applying (12) to (14), the equations of motion become

$$\rho\frac{\partial^2 u}{\partial t^2} = \mu\left(\frac{\partial^2 u}{\partial x^2}+\frac{\partial^2 u}{\partial y^2}\right)+\left(\frac{2\mu^2+3\lambda}{\lambda+2\mu}\right)\frac{\partial^2 u}{\partial x^2} + \left(\frac{2\mu\lambda}{\lambda+2\mu}\right)\frac{\partial^2 v}{\partial x\partial y}+\mu\frac{\partial^2 v}{\partial y\partial x} - 2\alpha\mu\frac{(3\lambda+2\mu)}{\lambda+2\mu}\frac{\partial T}{\partial x} \quad (15)$$

$$\rho\frac{\partial^2 v}{\partial t^2} = \mu\left(\frac{\partial^2 v}{\partial x^2}+\frac{\partial^2 v}{\partial y^2}\right)+\left(\frac{2\mu^2+3\lambda}{\lambda+2\mu}\right)\frac{\partial^2 v}{\partial y^2} + \left(\frac{2\mu\lambda}{\lambda+2\mu}\right)\frac{\partial^2 x}{\partial y\partial x}+\mu\frac{\partial^2 v}{\partial x\partial y} - 2\alpha\mu\frac{(3\lambda+2\mu)}{\lambda+2\mu}\frac{\partial T}{\partial y}. \quad (16)$$

The linearized temperature equation is:

$$\kappa\nabla^2 T - C_v\dot{T} - \alpha(3\lambda+2\mu)T_o(\dot{\varepsilon}_1+\dot{\varepsilon}_2+\dot{\varepsilon}_3) = 0. \quad (17)$$

We apply (12) and also neglect z-directed temperature gradients to obtain

$$\kappa\left(\frac{\partial^2}{\partial x^2}T+\frac{\partial^2}{\partial y^2}T\right) - \left(C_v+\alpha^2\frac{(3\lambda+2\mu)^2}{\lambda+2\mu}T_o\right)\dot{T} - 2\alpha\mu\frac{(3\lambda+2\mu)}{\lambda+2\mu}T_o\left(\frac{\partial\dot{u}}{\partial x}+\frac{\partial\dot{v}}{\partial y}\right) = 0. \quad (18)$$

In summary, (15)–(16) and (18) form a set of coupled linear equations in 2-D. In order to find Q, we solve for the unforced eigenmodes. The generalized eigenvectors contain u, v and T at every node.

C. Quality Factor Calculations for Typical MEMS Resonators

The thermoelastic Q values for several example MEMS resonators have been calculated. Table I introduces the resonator structures and the material parameters used. In Table II, we summarize the simulated Q values for the various structures. We compare simulated results to calculations based on (2) where applicable. We also compare to data reported in the literature. In some cases, the experimental data appears to have achieved the thermoelastic limit. For these devices, it is clear that structural modifications that can engineer a higher thermoelastic limit are warranted. In devices where the measured Q value is less than half the thermoelastic limit, investigation into and minimization of other damping mechanisms is warranted.

A polysilicon beam resonating in its fundamental flexural mode was simulated and compared to measurements [9]. In the experiments, the beam was actually part of a doubly clamped tuning fork, to minimize anchor damping. For a resonator operating at 0.57 MHz, the measured Q equaled 10 281. Zener's formula (2) predicts Q = 10 300, for the beam at 0.57 MHz and with $\tau = a^2/\pi^2 D_{th}$ ($a = 12\ \mu$m beam width in the direction of flexural motion, and $D_{\mathrm{th}} = \kappa/\rho C_{\mathrm{sp}}$). The simulations used only a single clamped beam, with dimensions matching the beam of the tuning fork. The simulated frequency was 0.63 MHz and the simulated TED Q = 10,211. This remarkable correlation between simulation results and experiments suggests that the flexural beam Q is limited by thermoelastic damping. Higher

TABLE I
SUMMARY OF PARAMETERS USED IN Q SIMULATION AND CALCULATIONS FOR A LONGITUDINAL RESONATOR

Resonator	Units	Flexural (2D)	Longitudinal (2D)	Longitudinal (3D)	Torsional (3D)	Flexural with slit (3D)
Material		polysilicon	silicon	$Si_{0.35}Ge_{0.65}$	silicon	polysilicon
Material Property References		[9]		[14], [24]		[9]
Critical Dimensions	μm	400x12x20	290x10x10	32x40x2.2	5.5x2x0.2	150x3.5x35
Young's modulus	*GPa*	157	180	155	180	157
Density	kg/m^3	2330	2330	4810	2330	2330
Specific Heat	*J/kg•K*	700	700	377	700	700
Thermal Conductivity	*W/m•K*	90	130	59	130	90
Thermal Expansion Co-efficient	*ppm/K*	2.6	2.6	4.3	2.6	2.6

TABLE II
SUMMARY OF SIMULATED Q VALUES FOR A SELECTION OF MEMS RESONATORS. SIMULATION RESULTS ARE COMPARED WITH CALCULATIONS BASED ON ZENER'S SINGLE-MODE APPROXIMATION AND MEASURED RESULTS REPORTED IN THE LITERATURE

Resonator	Simulated Frequency	Measured Frequency	Simulated Q	Analytical Q	Measured Q	Experimental Reference
Fixed-fixed beam 2D	0.63 MHz	0.57 MHz	10,300	10,300	10,281	Candler et al.[9]
Longitudinal 2D	15.3 MHz	14.7 MHz	1,650,000	n/a	170,000	Mattila et al [20]
Longitudinal 3D	70.5 MHz	74.4 MHz	366,000	n/a	2863	Quévy et al. [15]
Torsional 3D	4.4 MHz	5.6 MHz	2E8	n/a	3300	Evoy et al. [16]
Fixed-fixed beam 3D	1.27 MHz	1.15 MHz	26,000	n/a	5600	Abdolvand et al.[21]

thermoelastic Q might be achieved by geometry modifications as explored in [9] or by fabricating a given structure from different materials as explored in [6].

A $Si_{0.35}Ge_{0.65}$ capacitively actuated, longitudinal mode resonator was modeled and simulated based on geometry information provided in [15] and material properties reported in [14], [24]. 4 $\mu m \times 4$ μm anchors were included in the simulation, with fixed boundary conditions at the ends of the anchors. Quévy *et al.* report the Q measurement of 2863 for the fundamental longitudinal mode of a bar resonator. Equation (2) was not applied to calculate the analytical Q, since the derivation was for flexural modes only. We find that the TED Q is two orders higher than the measured Q. This suggests that thermoelastic damping, for the fundamental longitudinal mode, is not a significant contributor to the overall energy loss in this resonator. Other mechanisms, such as anchor damping, are being optimized by this group with tangible impact on Q being reported [25].

A second longitudinal resonator was also simulated. The device described in [20] is single crystal silicon, and its resonance length of 290 μm far exceeds its other dimensions. This resonator is also capacitively actuated and operates at 14.7 MHz. The measured Q is 170 000, while the simulated thermoelastic Q is an order of magnitude larger. This device also does not appear to be thermoelastically limited.

A paddle resonator operating in its torsional resonance was simulated. The simulation model was based on the nonmetalized SOI device described in [16]. Fixed-fixed boundary conditions were applied to the ends of the tethers. The simulated resonant frequency was about 20% lower than the measured torsional frequency. The value of Young's modulus used in the simulations was on the high end of values reported in [17], so is unlikely to explain the discrepancy. Analytical calculation of the torsional frequency using [18] given a total torsional stiffness of 9.4×10^{-12} N • m/rad for the beams, and a second moment of inertia of 1.3×10^{-26} kg • m^2 for the plate yields 4.3 MHz, within 3% of the simulated result. The discrepancy between the measured frequency and the theoretical frequencies may be the result of fabrication induced variations in the sample dimensions. Evoy *et al.* reported experimental Q values in the range of 3300 for room temperature measurements, while the simulations predict thermoelastic Q values of 200 million. The simulated result is consistent with the physical understanding that torsional deformations produce little or no volumetric expansion and should therefore have negligible thermoelastic damping.

Finally, the flexural mode polysilicon beam with a center opening described in [21] was simulated. The case with a beam length of 150 μm and width of 3.5 μm was considered. Since the material parameters of the device were not available, we used the polysilicon values of [9]. Though the center opening dimensions were not provided, the SEM indicated that the slit was extremely narrow. Using Comsol Multiphysics, the narrowest slit we were able to model was 0.1 μm wide, centered in the 3.5 μm beam width. The slit was also centered in the 35 μm beam height, spaced 2 μm from top and bottom. The measured Q was 5600, while the simulated TED limited Q was 26 000. This simulated Q dropped to 25 000 for a solid polysilicon beam at the same frequency. We also simulated a wider slit, and found that the Q went up to 26 200 for a slit 0.35 μm wide. This suggests that at this frequency, the polysilicon beam has a TED limited

Q that starts at 25 000 and can be increased with an increasingly wider slit. The experimental reference may have had a narrower slit than we were able to model, but the simulations were useful in bounding the TED limited Q between approximately 25 000–26 000, and in identifying the trend. The TED Q is about 4.5 times higher than the experimentally measured Q. Though the device does not appear to be TED limited, thermoelastic damping is clearly important in this device and can still be optimized.

III. Weakly Coupled Approach to TED Solutions

Thermoelastic damping in MEMS resonators can also be calculated via a weakly coupled approach proposed by Zener. This approach uses eigenvalue solutions to the uncoupled mechanical and thermal equations [8]. We show how to numerically implement Zener's approach so that structures more complicated than a solid beam can be studied. While the fully coupled numerical analysis of Section II is much more accurate, we emphasize that Zener's approach can offer design insights that might not otherwise be possible. Sections III–A–III–D describe the analysis. For simplicity, the formulas in this section are written for the 2–D case and use vector notations, with $\bar{u} = \begin{bmatrix} u \\ v \end{bmatrix}$, where u and v are the displacements in the x and y directions, respectively.

In Section III–A we introduce time-harmonic modal expansions for the mechanical and thermal domain solutions. Both the thermal modes and the mechanical modes of a given structure can be found numerically by eigenvalue analysis, assuming no thermoelastic coupling. Section III–A shows how to calculate the relative thermal mode amplitudes that are driven by the one mechanical mode. Sections III–B–III–C introduce two expressions for the energy loss per cycle. In Section III–B, the mechanical energy loss as a function of mechanical and thermal modes is derived. By energy conservation, this is equal to the energy transferred to the thermal domain. In Section III–C, the energy coupled into the thermal domain is taken directly from [8], where the net heat rise is derived in terms of the entropy generated per cycle. The expressions for energy lost per cycle in Sections III–B and III–C can be evaluated directly from the modal solutions obtained numerically. Though it is not obvious upon inspection that the two expressions are algebraically identical, energy conservation requires that they are equal. We have validated this numerically for isotropic solids, and [8] provides an algebraic proof for solids with cubic symmetry.

In Section III–E, we apply the weakly coupled formulation to the cases of a solid beam and two versions of a slotted beam. We describe insights gained by studying the modes obtained in the weakly coupled approach. In each example, we compare the Q value found with the Q calculated through a fully coupled analysis. A thorough experimental study of the slotted beam is referenced [9], where TED calculations are compared with experimental measurements over a wide range of frequencies.

A. Modal Solutions to Thermal and Mechanical Systems

Zener first identified the mechanical resonant mode of interest, and assumed a sinusoidal steady state of the form

$$\bar{u}(x,y,t) = \mathrm{Re}\left(U_m \bar{\Phi}_m(x,y) e^{j\omega_m t}\right). \tag{19}$$

This is the m^{th} eigensolution to the vector version of (15)–(16), without the thermal coupling term. $\bar{\Phi}_m(x,y)$ is a real valued modal shape function, U_m is the mode amplitude, and ω_m is the mechanical resonant frequency. Note that the shape functions and frequencies can be found numerically using either Comsol Multiphysics or another commercially available software package.

Spatial variations of strain caused by the mechanical vibration generate thermal gradients that are captured by the driven thermal equation.

$$\kappa \nabla^2 T - C_v \dot{T} = \theta_c T_o \nabla \cdot \dot{\bar{u}} \tag{20}$$

where θ_c captures the combination of constants written explicitly in (17), and where the term of order α^2 is neglected. For simplicity, we also limit our study to one mechanical mode at a time, $\bar{\Phi}_{\mathrm{mech}}$ and ω_{mech}

$$\kappa \nabla^2 T - C_v \dot{T} = \theta_c T_o \nabla \cdot \bar{\Phi}_{\mathrm{mech}} \left(U_{\mathrm{mech}} j\omega_{\mathrm{mech}} e^{j\omega_{\mathrm{mech}} t}\right). \tag{21}$$

This equation is solved as a function of the mechanical resonance amplitude U_{mech}. Applying separation of variables, the response to a drive at frequency ω_{mech} is

$$T(x,y,t) = T_0 + \mathrm{Re}\left(\sum_n A_n \mathrm{T}_n(x,y) e^{j\omega_{\mathrm{mech}} t}\right). \tag{22}$$

The functions $\mathrm{T}_n(x,y)$ are the real-valued spatial eigenmodes of the undriven thermal equation and A_n are the complex modal amplitudes. To find the modal amplitudes, we apply the orthogonality of the eigenmodes $\mathrm{T}_n(x,y)$. The expansion (22) is substituted into (21). Multiplying (21) by T_l and integrating over the volume, we obtain

$$A_n = \frac{j\omega_{\mathrm{mech}} U_{\mathrm{mech}} \theta_c T_o}{\kappa_n - j\omega_{\mathrm{mech}} C_n} \int_V \nabla \cdot \bar{\Phi}_{\mathrm{mech}} \mathrm{T}_n dV \tag{23}$$

with

$$\kappa_n = \int_V \mathrm{T}_n \kappa \nabla^2 \mathrm{T}_n dV \tag{24}$$

$$C_n = \int_V \mathrm{T}_n C_v \mathrm{T}_n dV. \tag{25}$$

The absolute magnitude of $|A_n/U_{\mathrm{mech}}|$ from (23) can be used to assess the effective coupling of mechanical modes into the thermal domain.

To calculate the mechanical quality factor, we first have to calculate the energy lost by the mechanical system per radian, or equivalently, the energy gained by the thermal system per radian.

B. Energy Lost From Mechanical Domain

The energy lost from the mechanical domain, per radian, is

$$\Delta W = \frac{1}{2\pi} \oint \left[\int \left(\sigma_1 \frac{d\varepsilon_1}{dt} + \sigma_2 \frac{d\varepsilon_2}{dt} + \sigma_6 \frac{d\varepsilon_6}{dt}\right) dV\right] dt \tag{26}$$

in 2–D, where $\sigma_3 = \sigma_4 = \sigma_5 = 0$. Stress in the above equation is expanded as a function of strain and temperature using (3). The strain is expressed in terms of the modal amplitude

and shape function. This expansion is further simplified by recognizing that only the temperature dependent terms produce nonzero integrals over one cycle. Integration over time yields

$$\Delta W = \sum_n \Delta W_n = \sum_n \frac{1}{2}\int_V [\theta_c \mathrm{Im}(A_n) T_n]\left[U_{\mathrm{mech}} \nabla \cdot \bar{\Phi}_{\mathrm{mech}}\right] dV \quad (27)$$

where each term in this sum ΔW_n corresponds to the energy dissipated by the n^{th} thermal mode.

The thermal component of stress that is out of phase with the strain damps the vibration and this term may be identified in the first bracket in (27). The second bracket is the strain.

C. Energy Transferred to Thermal Domain

The expression for energy gained by the thermal domain per cycle is derived in [8] to be

$$\Delta W = \frac{T_0}{2\pi} \oint \left[\int \left(T^{-1} \kappa \nabla^2 T\right) dV \right] dt. \quad (28)$$

The T^{-1} term is replaced by its Taylor expansion $1/T_0 - T/T_o^2$ where it is assumed that the driven modal amplitudes are small relative to the ambient temperature. Only the latter term in this expansion produces a nonzero integral over one cycle, so that

$$\Delta W \approx \frac{1}{2\pi} \oint \left[\int \left(\frac{T}{T_0} \kappa \nabla^2 T \right) dV \right] dt. \quad (29)$$

Where κ is the thermal conductivity in Joules/(Kelvin-second-meter). Expanding T using (22) and (23), it may be shown that (29) reduces to

$$\Delta W = \sum_n \Delta W_n = \sum_n \frac{1}{2} \frac{|A_n|^2}{\omega_{\mathrm{mech}} T_0} \kappa_n. \quad (30)$$

D. Weakly Coupled Quality Factor Calculation

The maximum stored energy in the 2–D mechanical system is given by

$$W = \frac{1}{2}\int_V (\sigma_1 \varepsilon_1 + \sigma_2 \varepsilon_2 + \sigma_6 \varepsilon_6) dV \quad (31)$$

where the integral is evaluated at the maximum mechanical amplitude.

This integral may be evaluated directly for a given mode shape by substituting (3) for stress with the appropriate 2–D approximations ($\sigma_3 = \sigma_4 = \sigma_5 = 0$). The Q of the device is then calculated by

$$Q^{-1} = \sum_n Q_n^{-1} = \sum_n \frac{\Delta W}{W} \quad (32)$$

where Q_n is an effective Q corresponding to the nth thermal mode. In applying (32) to calculate Q, ΔW can be found from either (27), the expression for mechanical energy lost, or (30), the thermal energy gained. These expressions can be shown to be equivalent.

This analysis shows that we can use numerically calculated modal solutions of uncoupled thermal and mechanical equations to calculate the Q. For simplicity, we restricted our analysis to a single mechanical mode of interest. We considered that possibly many thermal modes would contribute to damping in the system. The individual terms in the sum (32) for Q can be used to identify the thermal modes that contribute most to damping and evaluate their relative weights.

E. Using Weighting Functions to Optimize a UHF Beam Resonator

Fig. 1 shows the calculated Q values for a range of thermal modes in a beam. The beam is assumed to be in its fundamental flexural resonance, at frequency 0.63 MHz. The frequency and mode shape were found numerically. The first forty thermal modes were also found numerically. Using the approach described in Sections III–A–III–D, we evaluated the thermoelastic damping associated with each mode. The Comsol Multiphysics module was used to evaluate the overlap integrals in $|A_n|$ (23) that are needed to evaluate ΔW in (27) or (30). The total Q, based on forty modes in (32), was found to be 10 400. The Q calculated in a full TED simulation as described in Section II–B was 10 200. The weakly coupled calculations show that this damping is dominated by the contribution of a single mode, whose thermal eigenfunction is shown in the inset. This mode at 0.605 MHz gave $\mathrm{Q} = 11\,000$. Interestingly, the temperature distribution of this mode is not uniform along the beam axis. Though Zener's original approximation assumed that dominant thermal mode had no variation along the beam axis, we find that the uniform mode, also shown in Fig. 1, has a high $\mathrm{Q} = 6\,250\,000$.

After observing the thermal distribution of the dominant thermal mode, we consider the effect of placing slots in the beam. The slots, proposed originally in [9], are designed to alter the dominant thermal mode without significant effect on the fundamental flexural mode frequency. Fig. 2 shows plots the Q_n values for the solid beam from Fig. 1 next to the results for a slotted beam. The slots had the effect of modifying the thermal eigensolutions and characteristic frequencies. In the slotted beam, many more thermal modes contribute to the damping of the structure. On the other hand, the thermal modes with the greatest spatial overlap are moved to much higher frequencies, minimizing their overall effect on damping. In this beam, the slots had the effect of raising the total Q value by a significant factor of 4.

If the mechanical mode frequency were already much higher than the dominant thermal mode, then moving the dominant modes up in frequency could have a detrimental effect on Q. This case is shown in Fig. 3. Originally, in the solid beam, the mechanical frequency is at 4.327 MHz, while the dominant thermal mode is still at 0.605 MHz. When slots are added to

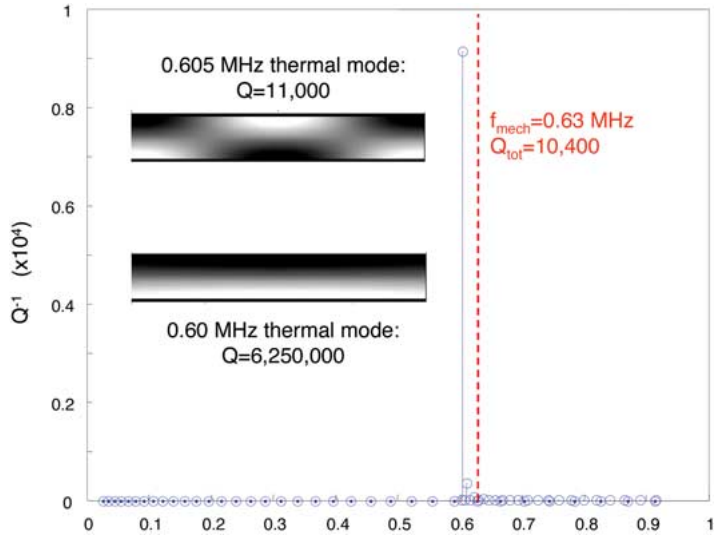

Fig. 1. Q values for thermal modes in a fixed-fixed, thermally insulated beam that is 400 μm long and 12 μm wide. The mechanical resonance is the fundamental flexural mode at 0.63 MHz. The first 40 thermal modes are calculated. The three most heavily damped modes are: at 0.6 MHz with a Q of 6 250 000; at 0.605 MHz with a Q of 11 000; and at 0.611 MHz with a Q of 280 000 (spatial profile not shown in inset). The total device Q, including all 40 thermal modes is 10 400.

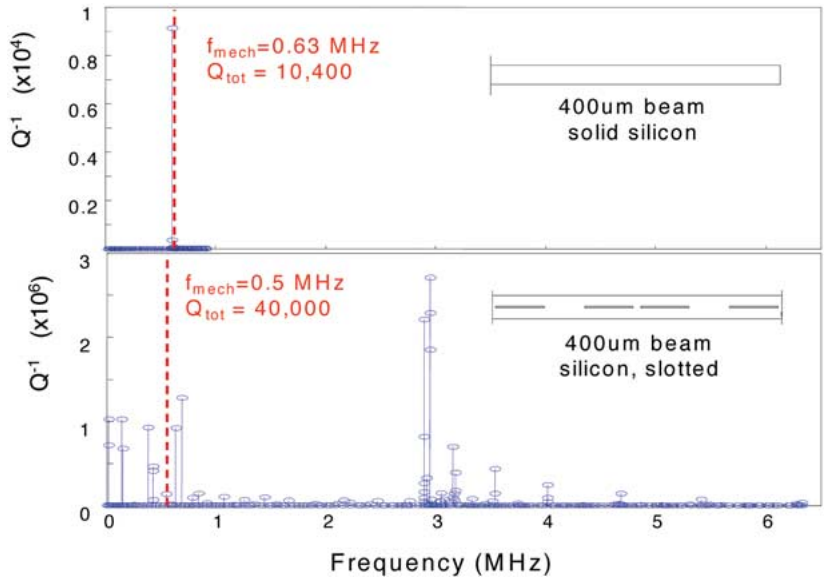

Fig. 2. Q values for thermal modes in a fixed-fixed, thermally insulated beam that is 400 μm long and 12 μm wide. The top plot shows the solid beam thermal modes and mechanical resonance, while the bottom plot shows the same beam with 1 μm wide slits along the beam length. The effect of the slits on the thermal modes and their Q values indicated. The mechanical resonance shifts slightly, as expected. The total Q value is higher in the beam with slits.

this beam, thermal modes with significant spatial overlap move up in frequency, much nearer to the mechanical resonance. This lowers the Q to 20 200 from 38 000 without slots.

Since it is not always possible to predict the most relevant thermal mode and its time constant intuitively, the numerical approach can be extremely helpful. We see that simple modifications to the resonator can have the effect of completely altering the thermal mode structure and introducing complicated weightings in the Q calculation. Both the frequency and the spatial overlap of the thermal modes are clearly important. When modes that have high spatial overlap are also close to the mechanical resonance frequency, large thermoelastic damping results. Since structural modifications that have a beneficial impact in some frequency regimes can be detrimental in others, engineering to optimize Q can be greatly enabled through the use of the numerical approach described here.

IV. Conclusion

This paper presented two new tools to evaluate and optimize MEMS structures for low thermoelastic damping. The weakly coupled approach is based on original work by Zener. We reviewed Zener's approach and showed how numerical finite elements based approaches can be used to fully leverage Zener's theory. In the weakly coupled approach, the fundamental thermodynamic energy expressions are coupled. However the strain and temperature solutions used to evaluate these energies are taken from solutions to uncoupled, standard mechanical and thermal equations. This allows us to use readily available finite

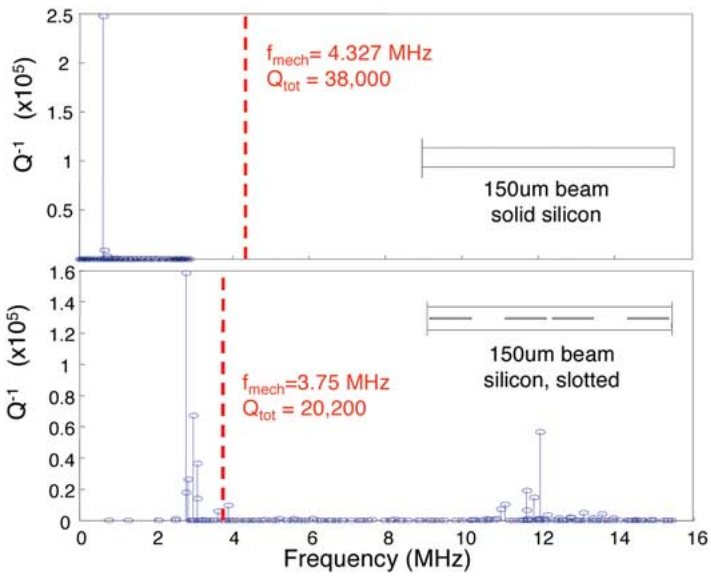

Fig. 3. Q values for thermal modes in a fixed-fixed, thermally insulated beam that is 150 μm long and 12 μm wide. The top plot shows the solid beam thermal modes and mechanical resonance, while the bottom plot shows the same beam with 1 μm wide slits along the beam length. The effect of the slits on the thermal modes and their Q values indicated. The mechanical resonance shifts slightly, as expected. The total Q value is lower in the beam with slits.

elements packages and evaluate thermoelastic damping. The approach enables a great deal of insight into the energy loss mechanism. We find that a spatial overlap of thermal modes with the strain profile in the mechanical mode of interest is a dominant term in the damping. In addition, the frequency separation between relevant thermal modes and the mechanical resonance frequency must be considered. By studying the damping contributions of individual thermal modes, their mode shapes, and their frequencies, it is possible to engineer MEMS resonators for higher Q. In addition, by reviewing the fundamental coupled thermodynamic energy expressions, we achieve a greater insight into the energy loss mechanism itself.

Finally, this paper outlines a method for solving the fully coupled thermoelastic dynamics to obtain exact expressions for Q in an arbitrary resonator. The fully coupled simulations enable a precise evaluation of Q. We derive both 3-D equations, as well as 2-D plane stress thermoelastic equations. The simulations were conducted in Comsol Multiphysics. This software can parameterize the material parameters and geometry, so that detailed optimization studies are enabled. We showed that the fully coupled simulations predict thermoelastically limited Q in structures reported in the literature.

ACKNOWLEDGMENT

The authors would like to thank M. Mescher and E. Carlen of Draper Laboratory, as well as S. Chandorkar and Professor K. Goodson of Stanford University for valuable conversations. They also thank N. Barbour and J. McElroy for support at Draper and Dr. C. Nguyen.

REFERENCES

[1] R. Lifshitz and M. Roukes, *Phys. Rev. B*, vol. 61, no. 8, p. 61, 2000.
[2] B. H. Houston, D. M. Photiadis, M. H. Marcus, J. A. Bucaro, X. Liu, and J. F. Vignola, *Appl. Phys. Lett.*, vol. 80, no. 7, pp. 1300, 2002.
[3] T. V. Roszhart, "Micromachined silicon resonators," in *Electro Int.*, 1991.
[4] V. T. Srikar and S. D. Senturia, "Thermoelastic damping in fine-grained polysilicon flexural beam resonators," *J. Microelectromech. Syst.* , vol. 11, no. 5, pp. 499–504, 2002.
[5] R. Abdolvand *et al.*, "Thermoelastic damping in trench-refilled polysilicon resonators," in *Proc. Transducers, Solid-State Sensors, Actuators and Microsyst., 12th Int. Conf.*, 2003.
[6] A. Duwel, J. Gorman, M. Weinstein, J. Borenstein, and P. Ward, *Sens. Actuators A*, vol. 103, pp. 70–75, 2003.
[7] C. Zener, "Internal friction in solids: I. Theory of internal friction in reeds," *Phys. Rev.*, vol. 52, p. 230, 1937.
[8] ——, "Internal friction in solids: II. General theory of thermoelastic internal friction," *Phys. Rev.*, vol. 53, p. 90, 1938.
[9] R. N. Candler, M. Hopcroft, W.-T. Park, S. A. Chandorkar, G. Yama, K. E. Goodson, M. Varghese, A. Duwel, A. Partridge, M. Lutz, and T. W. Kenny, "Reduction in thermoelastic dissipation in micromechanical resonators by disruption of heat transport," in *Proc. Solid State Sens. Actuators*, 2004, pp. 45–48.
[10] A. S. Nowick and B. S. Berry, *Analastic Relaxation in Crystalline Solids*. New York: Academic, 1972, ch. 17.
[11] Comsol Multiphysics is a product of Comsol, Inc. [Online]. Available: http://www.comsol.com
[12] G. John, "Finite element model of thermoelastic damping in MEMS," M.S., Mass. Inst. Technol., Dep. Mater. Sci., , 2002.
[13] B. Antkowiak, J. P. Gorman, M. Varghese, D. J. D Carter, and A. Duwel, "Design of a high Q low impedance, GHz-range piezoelectric resonator," in *Proc. Transducers, Solid-State Sensors, Actuators and Microsyst., 12th Int. Conf.*, 2003.
[14] F. Schaffler, *Properties of Advanced SemiconductorMaterials GaN, AlN, InN, BN, SiC, SiGe*, M.E. Levinshtein, S.L. Rumyantsev, and M.S. Shur, Eds. New York: Wiley, 2001, pp. 149–188.
[15] E. P. Quévy, S. A. Bhave, H. Takeuchi, T.-J. King, and R. T. Howe, "Poly-SiGe high frequency resonators based on lithographic definition of nano-gap lateral transducers," in *Proc. Solid State Sens. Actuators*, 2004, pp. 360–363.
[16] S. Evoy, A. Olkhovets, L. Sekaric, J. M. Parpia, H. G. Craighead, and D. W. Carr, "Temperature-dependent internal friction in silicon nanoelectromechanical systems," *Appl. Phys. Lett.*, vol. 77, no. 15, pp. 2397–2399, 2000.
[17] [Online]. Available: http://www.memsnet.org
[18] Roark and Young, *Formulas for Stress and Strain*. New York: McGraw-Hill, 1975.
[19] Nowacki, *Thermoelasticity*. Elmsford, NY: Pergamon, 1962.
[20] T. Mattilia, A. Oja, H. Seppä, O. Jaakkola, J. Kiihamäki, H. Kattelus, M. Koskenvuori, P. Rantakari, and J. Tittonen, "Micromechanical bulk acoustic wave resonator," in *IEEE Ultrason. Symp.*, 2002, p. 945.

[21] R. Abdolvand, G. Ho, A. Erbil, and F. Ayazi, "Thermoelastic damping in trench-refilled polysilicon resonators," in *Proc. Transducers, Solid-State Sens., Actuators and Microsyst., 12th Int. Conf.*, 2003.
[22] Hao and Ayazi, "Thermoelastic damping in flexural mode ring gyroscopes," in *2005 ASME*, Orlando, FL, Nov. 5-11, 2005.
[23] D. S. Bindel and S. Govindjee, "Elastic PMLs for resonator anchor loss simulation," *Int. J. Numer. Meth. Eng.*, vol. 64, no. 6, pp. 789–818, Oct. 2005.
[24] S. A. Bhave, B. L. Bircumshaw, W. Z. Low, Y.-S. Kim, A. P. Pisano, T.-J. King, and R. T. Howe, "Poly-SiGe: A high-Q structural material for integrated RF MEMS," in *Solid-State Sensor, Actuator and Microsystems Workshop*, Hilton Head Island, SC, Jun. 2-6, 2002.
[25] D. S. Bindel, E. Quévy, T. Koyama, S. Govindjee, J. W. Demmel, and R. T. Howe, "Anchor loss simulation in resonators," in *18th IEEE Microelectromechan. Syst. Conf. (MEMS-05)*, Miami, FL, Jan.-Feb. 30-3, 2005.

Amy Duwel received the B.A. degree in physics from the Johns Hopkins University, Baltimore, MD, in 1993. She received the M.S. and Ph.D. degrees in 1995 and 1999, respectively, in electrical engineering and computer science from the Massachusetts Institute of Technology (MIT), Cambridge.

She is currently the MEMS Group Leader, Charles Stark Draper Laboratory, Cambridge, and a Principal Member of the Technical Staff. Her technical interests focus on microscale energy transport, and on the dynamics of MEMS resonators in application as inertial sensors, RF filters, and chemical detectors.

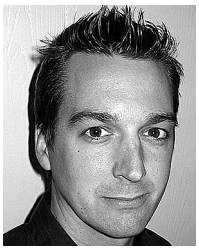

Rob N. Candler received the B.S. degree in electrical engineering from Auburn University in 2000 and the M.S. and Ph.D. degrees in electrical engineering from Stanford University, Stanford, CA, in 2002 and 2006, respectively.

His research interests include energy loss mechanisms in micromechanical resonators, MEMS packaging, and sensor networks.

Thomas W. Kenny received the B.S. degree in physics from the University of Minnesota, Minneapolis, in 1983 and the M.S. and Ph.D. degrees in physics from the University of California, Berkeley, in 1987 and 1989, respectively.

From 1989 to 1993, he was with the NASA Jet Propulsion Laboratory, where his research focused on the development of electron-tunneling high-resolution microsensors. In 1994, he joined the Mechanical Engineering Department, Stanford University, Stanford, CA, where he directs MEMS-based research in a variety of areas including resonators, wafer-scale packaging, cantilever beam force sensors, microfluidics, and novel fabrication techniques for micromechanical structures. He is a founder and CTO of Cooligy, a microfluidics chip cooling components manufacturer, and founder and board member of SiTime, a developer of CMOS timing references using MEMS resonators. He has authored and coauthored more than 200 scientific papers and holds 40 patents.

Dr. Kenny is presently the Stanford Bosch Faculty Development Scholar and the General Chairman of the 2006 Hilton Head Solid State Sensor, Actuator, and Microsystems Workshop.

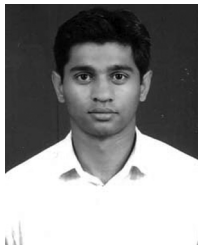

Mathew Varghese received the B.S degree in electrical engineering and computer science with a minor in physics from the University of California, Berkeley. He received the S.M. and Ph.D. degrees in electrical engineering and computer science from the Massachusetts Institute of Technology (MIT), Cambridge, in 1997 and 2001, respectively.

Currently, he heads the Microsystems Integration Group and is a Principal Member of Technical Staff with the Charles Stark Draper Laboratory, Cambridge. His research interests focus on the fabrication, design, and analysis of microsystems. He has led projects to build microphones, drug delivery devices, MEMS RF filters, and Chip Scale Atomic Clocks (CSAC).

Dr. Varghese won a Distinguished Performance award for leading the CSAC development effort at Draper.